MEASUREMENT OF CHANGE IN CTE OF PCBS DUE TO SINGLE PHASE IMMERSION COOLING AND IMPACT OF CHANGED PROPERTIES OF PCBS ON SOLDER JOINT RELIABILITY OF BGA PACKAGE

by

SAMEER HEMANT DHANDARPHALE

THESIS

Submitted in partial fulfillment of the requirements
for the degree of Master of Science in Mechanical Engineering at
The University of Texas at Arlington
May 2020

Arlington, Texas

Supervising Committee:

Prof. Dereje Agonafer, Supervising Professor
Prof. A. Haji-Sheikh
Prof. Amir Ameri
Dr. Fahad Mirza

Acknowledgements

I would like to thank Dr. Agonafer for his guidance and for giving me opportunity to work in reliability lab. I would also like to thank Dr. Haji-Sheikh, Dr. Amir Ameri and Dr. Fahad Mirza for being on my thesis committee.

I appreciate guidance and help of my mentors and colleagues Tushar, Abel, Raufur, Rabin, Akshay and Mehzabeen.

April 27th, 2020

Abstract

MEASUREMENT OF CHANGE IN CTE OF PCBS DUE TO SINGLE PHASE IMMERSION COOLING AND IMPACT OF CHANGED PROPERTIES OF PCBS ON SOLDER JOINT RELIABILITY OF BGA PACKAGE

Sameer Hemant Dhandarphale, M.S.

The University of Texas at Arlington, 2020

Supervising Professor: Dr. Dereje Agonafer

Oil immersion cooling in high-density data centers is emerging as an alternative for traditional air cooling because of the less power consumption, capacity to handle high power density and less space requirement. To adopt this technique extensively, effect of immersion on reliability of server components in dielectric coolant needs to be evaluated. One of the major reliability concerns in BGA package is 2nd level solder joint failure. The primary reason of solder joint failure is CTE mismatch between the PCB and the package. Also, difference in stiffness of the PCB and the package affects the solder joint reliability. As properties of the PCB change after immersion of PCB in dielectric coolant, it affects the reliability of solder joint. In this thesis, samples of PCBs 185HR/370HR are immersed in dielectric fluid EC100 for the period of 720 hours. The changes in CTE are calculated using Thermo- Mechanical Analyzer (TMA). Solder joint reliability is studied for after and before immersion of PCB in dielectric coolant for BGA package using FE Analysis under thermal cycling.

Table of Contents

List of Figures

List of Tables

Chapter 1

Introduction

1.1 Data Center

Data center is a facility where organization's data is stored, managed and disseminated in form of IT equipment and operations. Data centers are heart of the network and daily operations. Providing 24/7 access to operations makes data centers one of the most energy consuming facilities in the world. The IT equipment include servers, storage hardware, cables, racks and firewalls.[1]

The large amount of this data is stored, managed and disseminated in data centers in form of IT equipment and operations. Data centers are heart of the network and daily operations.

By the year 2020, more than 50 billion devices will be connected to the internet and will generate more than 44 ZB data per year. Hence there is a need for more computing performance for increased requirements which will result in more power consumption.[2]

1.2 Data Center Power Consumption

The capacity of data center is given by power density. Power density is used to be measured in W/sqft , but now it is measured in kW/rack. 2 to 4 kW/rack was once considered as high density, but it has changed to 10 to 12 kW/rack by 2016. Typically, a high density setup is one using more than 150 W/sqft. 2/3rd of data centers in US are experiencing higher peak densities around 15 to 16 kW/rack. [9]

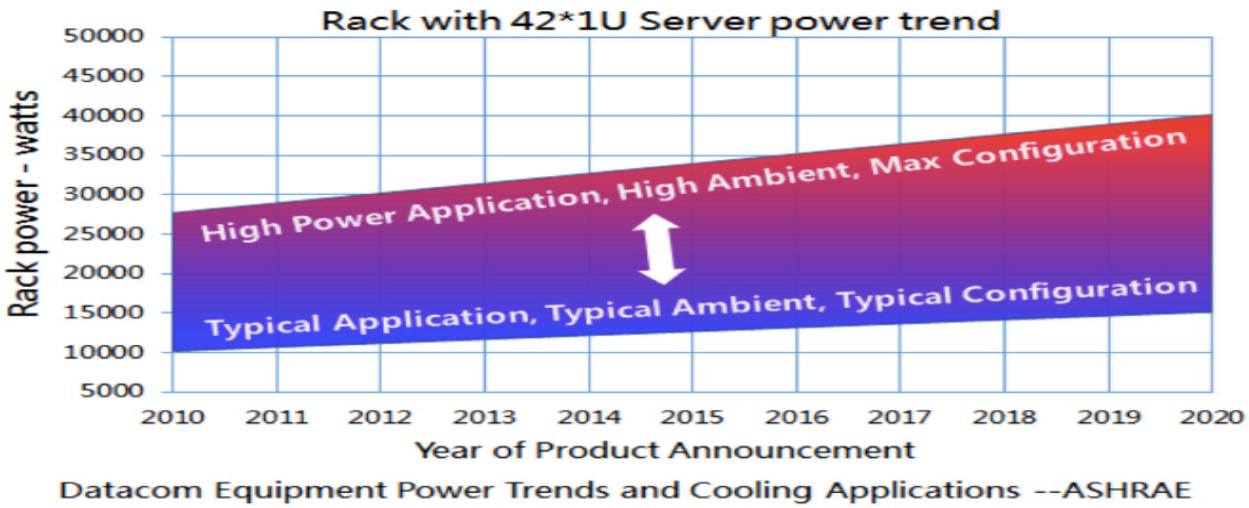

Figure 1 Increase in Rack Power in Recent Years

That is why one of the main concerns in data center facilities is very large energy consumption. Conventional air cooling is not able to meet the heat dissipation demands at acceptable cost. Hence organizations have been looking into using more efficient technologies and practices in data center.

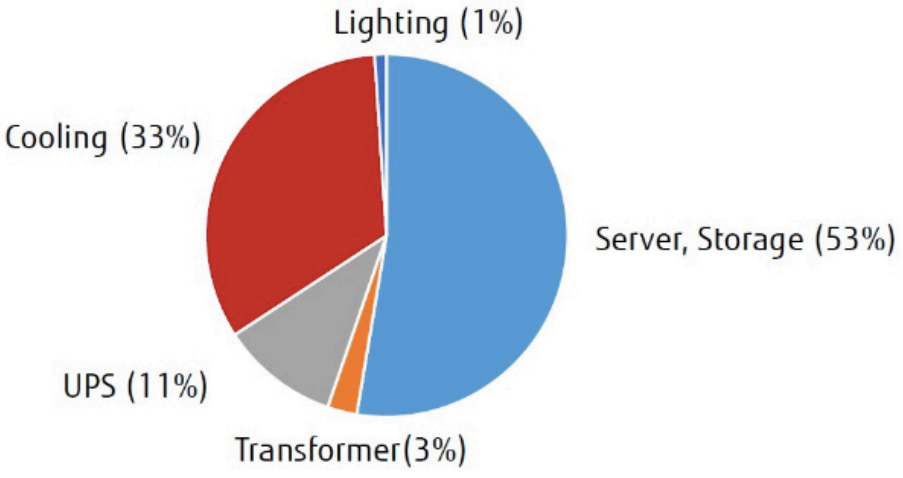

A Shehabi: LAWRENCE BERKELEY NATIONAL LABORATORY "United States Data Center Energy Usage Report", 2016.

Figure 2 US Data Center Energy Report

Data center efficiency is often determined in terms of Power Usage Effectiveness (PUE). It is given by

$$\text{Data Center PUE} = \frac{\text{Total Data Center Power kW}}{\text{Total IT Power kW}}$$

According to Uptime Institute survey of over 1100 data centers, average PUE of a data center is around 1.8-1.89.

Following graph shows average PUE using various cooling techniques.

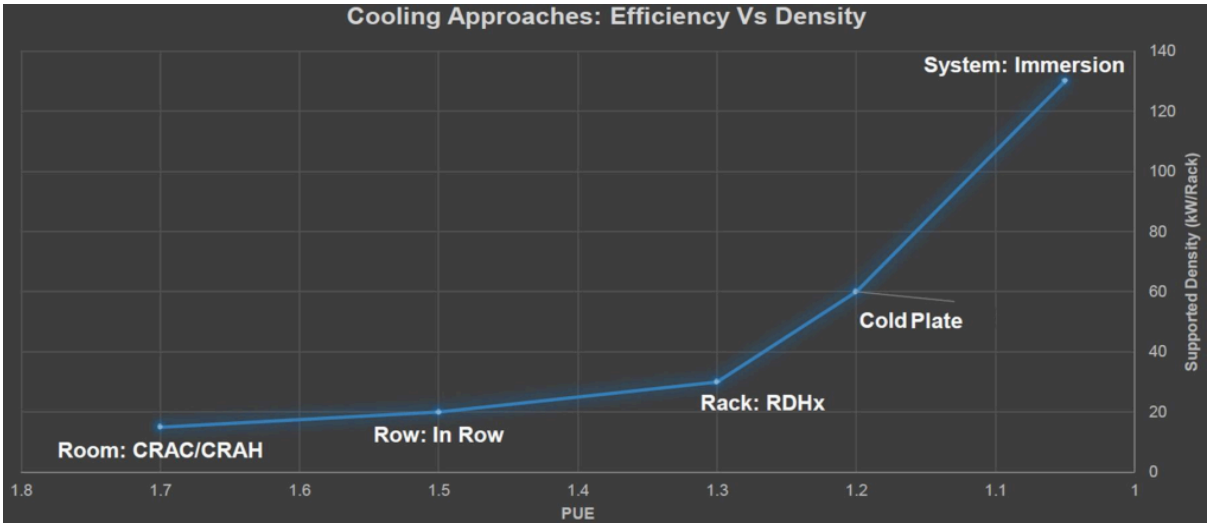

Figure 3 PUE for Different Cooling Approaches [1]

1.3 Rising Insufficiency of Air-Cooling in Case of High Density Data Centers

Air cooling is most popular cooling technique. But as power requirement is increasing day by day, air cooling has started to show it's limitations. As shown in the fig 4, air cooling consumes significant i.e around 33% of total power usage. Also, air-cooling results into massive carbon footprint. Some of the other advantages can be listed as, it is expensive to maintain. Fans and other components often fail. Surrounding

atmospheric conditions have great impact on the working and efficiency. Air pollutants and condensation on equipment can damage hardware.

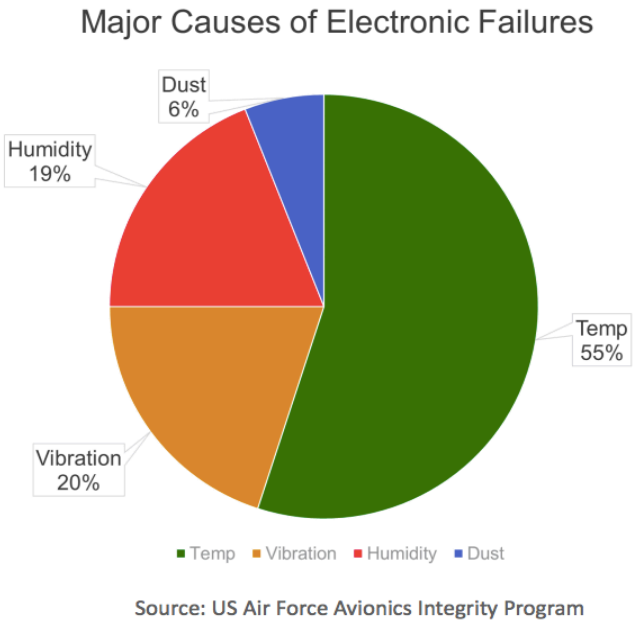

Figure 4 Causes of Electronic Failures

The air-cooling technique is about to come at a stage where there is very low scope for the improvement. First of all, with increase in heat density, air becomes less efficient coolant.

To increase the efficiency, total power consumption should be reduced. Potential contributing factors are;

1) Compressors/heat exchangers (better h_w, ΔT)

2) Pumps (reducing speed, reducing mass)

3) Fans (better h_w, reducing speed)

4) Better coolant media (lower air temp)

5) Effective air flow paths [10]

As these all factors are almost at the peak of their effectiveness and efficiency. It is time to consider alternative options.

1.4 Liquid Cooling

Liquid Cooling demonstrates its advantages in high density facilities, which require more effective and efficient cooling for more powerful and dense hardware. The energy dedicated to liquid cooling can be recovered and recycled reducing or even eliminating its carbon footprint.

1.4.1 Immersion Cooling

Liquid immersion cooling is an innovative type of electronic cooling techniques in which the racks are completely immersed in a dielectric coolant. The heat is transferred directly from the heat source to the circulating liquid coolant and then from coolant to heat exchanger. Liquid coolant is circulated at very low pressure and very low flow rates.

Liquid Cooling demonstrates its advantages in high density facilities, which require more effective and efficient cooling for more powerful and dense hardware. The energy dedicated to liquid cooling can be recovered and recycled reducing or even eliminating its carbon footprint.

Liquid immersion cooling gives better cooling capacity and lower PUE than conventional cooling techniques like CRAC or CRAH. As fans, chillers or similar hardware are not required, less opex, better energy efficiency, noise reduction is achieved.[5]

The main reason liquid cooling is more effective than air cooling is that the thermal resistance can be reduced drastically because of liquid as a medium.

$$Q_{Load} = mC_p\Delta T = rVC_p\Delta T$$

1.4.2.1 Single Phase Immersion Cooling

In single-phase immersion cooling, the coolant does not undergo phase change i.e always stays in liquid state. The boiling temperature of the coolant is higher than maximum working temperature of the system. For single phase immersion cooling, open bath system is used as there is little or no risk of fluid evaporation. The fluid is circulated in the system using the pump. Heat is absorbed from the coolant by heat rejection devices such as radiator, dry cooler, liquid-to-liquid heat exchanger, or cooling tower.[7]

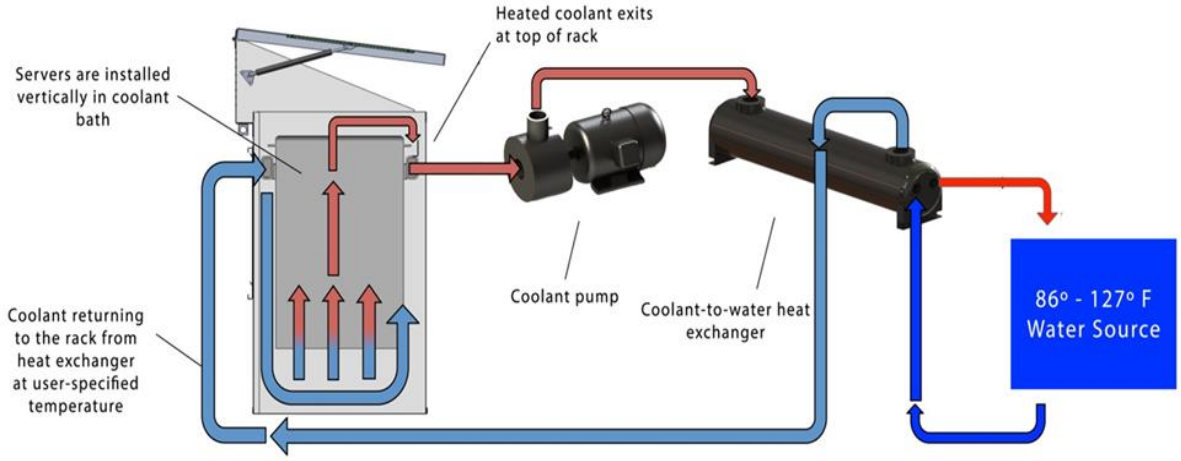

Figure 5 Schematic of Working of Single Phase Immersion Cooling [3]

1.4.2.2 Two Phase Immersion Cooling

Two-phase passive immersion cooling exponentially increases heat transfer efficiency from boiling and condensation of cooling fluids. Electronic components are submerged in non-conductive liquid bath in an accessible sealed enclosure [10].

Heat is removed when fluid comes in direct contact with chip or other heat source. This results in fluids reaching their boing temperature and fluid is converted in vapor. The vapor formed travels to top of the enclosure. There it comes in the contact with condensation coil and is again transferred

into the liquid state and falls back into the bath. This cycle is repeated over and over again. The liquid coolants used in two phase cooling have low boiling temperature and low latent heat [4][8].

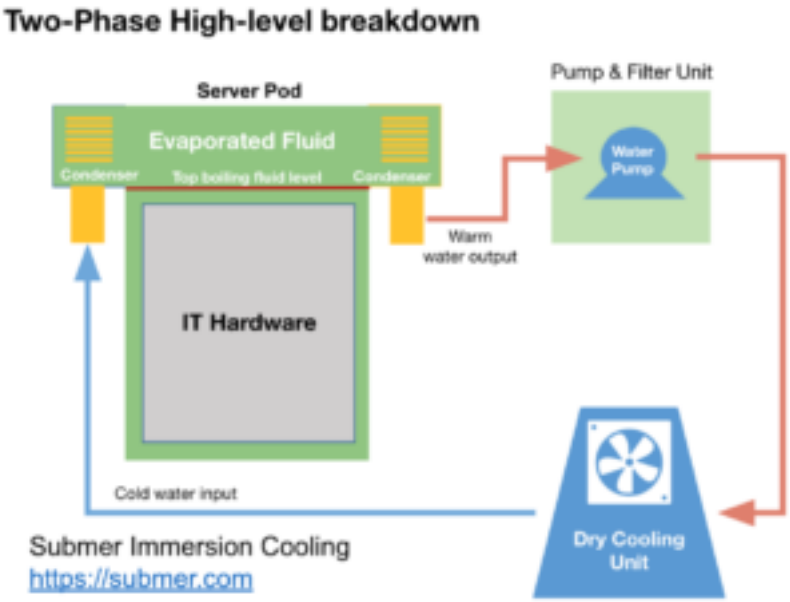

Figure 6 Schematic of Working of Two-Phase Immersion Cooling

1.4.3 Challenges

Changes in thermo mechanical properties of components after immersion which are important to predict long term reliability are unknown. Hence even though oil immersion cooling is efficient than conventional cooling techniques, there is still hesitation in industry to use liquid immersion cooling. As the heat sinks will not be an efficient option, there is need of appropriate material to spread over the heat surface to improve the heat dissipation. As the requirements of data centers using immersion cooling are different than the one's using air cooling, new architecture of servers and overall data centers should be developed. Optimum designs of tank sealing, space utilization, monitoring and management systems should be developed. Effect of liquid immersion on performance of CPU and different components should be evaluated. As liquid is dense than air, there will be limitations on use of optical devices.[5]

1.5 BGA Package

Ball Grid Array Package is a type of surface mount technology packages. In BGA, solder balls are used as interconnects between PCB and IC. These solder balls arranged in a grid pattern. Instead of perimeter, the bottom surface area of the package is used for interconnections. Package is placed the top of PCB. Assembly is kept in reflow oven or infrared heater to melt assembly solder balls and hence to create strong metallurgical bond at both ends of the interconnect. Due to the surface tension, package is aligned with solder ball [12][13].

BGA package provides advantages such as excellent thermal compatibility and improved current distribution. The main disadvantage of BGA package is the difficulty to inspect for soldering faults [13].

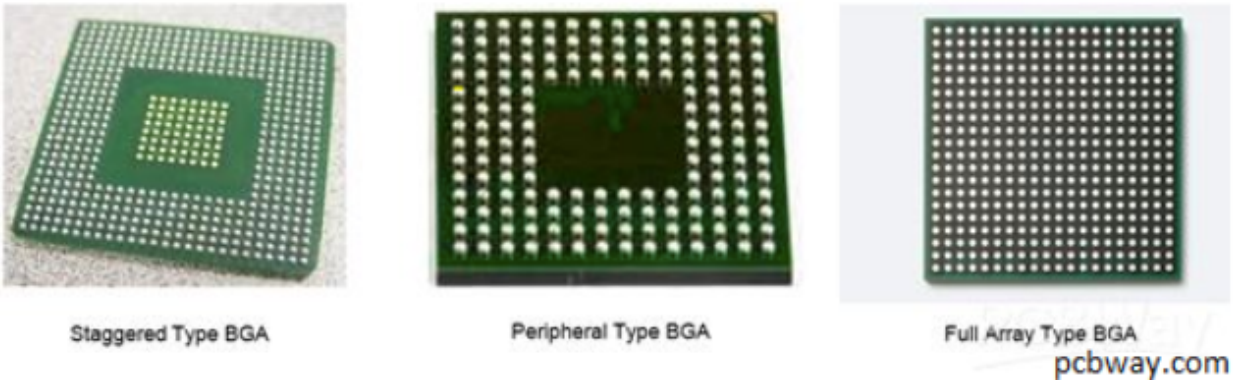

Figure 7 BGA Packages

1.6 Board Level Reliability

One of the definitions of reliability is the ability of a component or a system to perform its functions upto certain efficiency level under certain conditions and duration. To estimate the reliability of

package or its components, reliability tests are adapted, documented and standardized by Joint Electronic Device Engineering Council (JEDEC) and Institute for Printed Circuits (IPC) [11]. Mismatch between coefficient of thermal expansion (CTE) of various package components is one of the biggest reliability concerns in electronic packages. CTE mismatch causes warping and uneven expansion of the package. This results into generation of internal thermal stresses and thus the crack initiation and propagation. Thermal cycling tests are most common reliability tests used to observe themo-mechanical behavior of components.

Reliability tests can be broadly classified into two types; (a) Package Level (b) Board Level. Package level reliability tests focus on robustness of the components and package design to withstand required environmental conditions. Board level reliability tests focus on stresses developed at different locations, especially at the interconnects [11][12].

1.7 Solder Interconnects

Due to uneven expansion of package components and PCB due to CTE mismatch, internal stresses are developed on solder balls. Especially at high temperatures, possibility of solder joint failure is

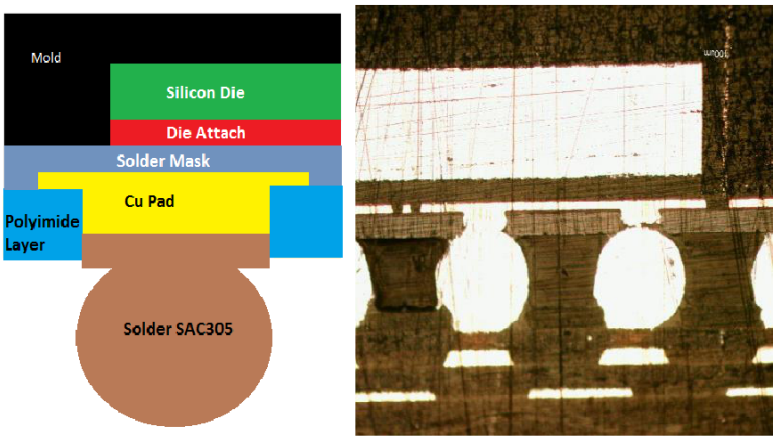

Figure 8 Figure 8 (a)Schematic of Solder Interconnect (b)Optical Microscopic Image [12]

high. The stiffness of PCB is considerably higher than that of package which also affects the solder joint reliability. Deshpande et. al. [18] have investigated the differences in fatigue life of solder joints under room temperature cyclic tensile and shear loads. Solder joints were found to fail earlier under tensile loads than shear loads. The general observation is critical solder ball joint either corner solder ball which has maximum distance from center or the solder ball underneath the end portion of die [12].

1.8 Motivation and Objective

One of the biggest challenges to adopt single phase liquid immersion cooling is lack of data on long term effects and hence reliability of immersed components. CTE mismatch between the PCB and the package has big impact on solder joint reliability especially at high temperatures. This study provides and compares CTEs of two different PCBs for three different cases; pre-immersion, post-immersion room temperature and post immersion thermal aging. Simulations were performed to evaluate and compare impact of change in CTE and Young's Modulus after immersion with before immersion.

Chapter 2

Material Characterization

2.1 Overview

PCB samples 185HR and 370HR were cut in 7mm*7mm samples using high speed cutter. Theses samples were immersed for 720 hours under two different conditions. Using TMA, CTE of these samples were measured for temperature range of 25°C to 200°C. Shrinath et. al [17] have used the same types of PCB samples to calculate Complex Modulus using Dynamic Mechanical Analyzer (DMA).

2.2 Thermo-Mechanical Analyzer (TMA)

Basic function of TMA is to measure change in z-direction as a function of Temperature. Using TMA, we can measure different thermal properties such as CTE (Coefficient of Thermal Expansion), glass transition temperature, melting point, etc. There are three types of probes used in this measurement based on the material properties; compression probe, tensile probe and penetration probe. Also, there are different types of probe materials. Most commonly used are; quartz, alumina and metal probes. Types of fixtures for expansion are three point bending or flexure, parallel plate fixture and penetration fixture. To detect change in length, LVDT (Linear Variable Differential Transformer) is used. LVDT is an inductive transducer. Typical temperature range of TMA is -150°C to 600°C [14].

Table 1 TMA SS6100 Specifications

Module	**TMA/ SS6100**
Unit Composition	TMA/SS6000 Base Unit+100H Heater+ Measurement unit
Heater type	100H Heater
Connected Sample tube	Quartz, K thermocouple
Connected Probe	Quartz
Probe Support	Cantilever
TMA Range (Sensitivity)	±5 mm
Program Speed	0.01 to 100 C/ min
Sample Length	Auto measurement

Measurement Physics: Sample is kept vertically under the compression probe in the test tube. Probe is connected to LVDT and force generator. Probe is touched to the sample to calculate the length and then to calculate displacement and to generate the force during the test. Test tube is enclosed by the furnace. Thermocouples are placed inside the test tube to calculate the sample temperature and furnace temperature.

In this experimental setup, quartz probe is used because of its low CTE. The temperature range for this setup is from 25°C to 250°C with temperature increment of 2°C/min. Sample size taken was 7mm*7mm and these sample were cut by high speed cutter. Three tests were performed for each experiment and their average value was taken.

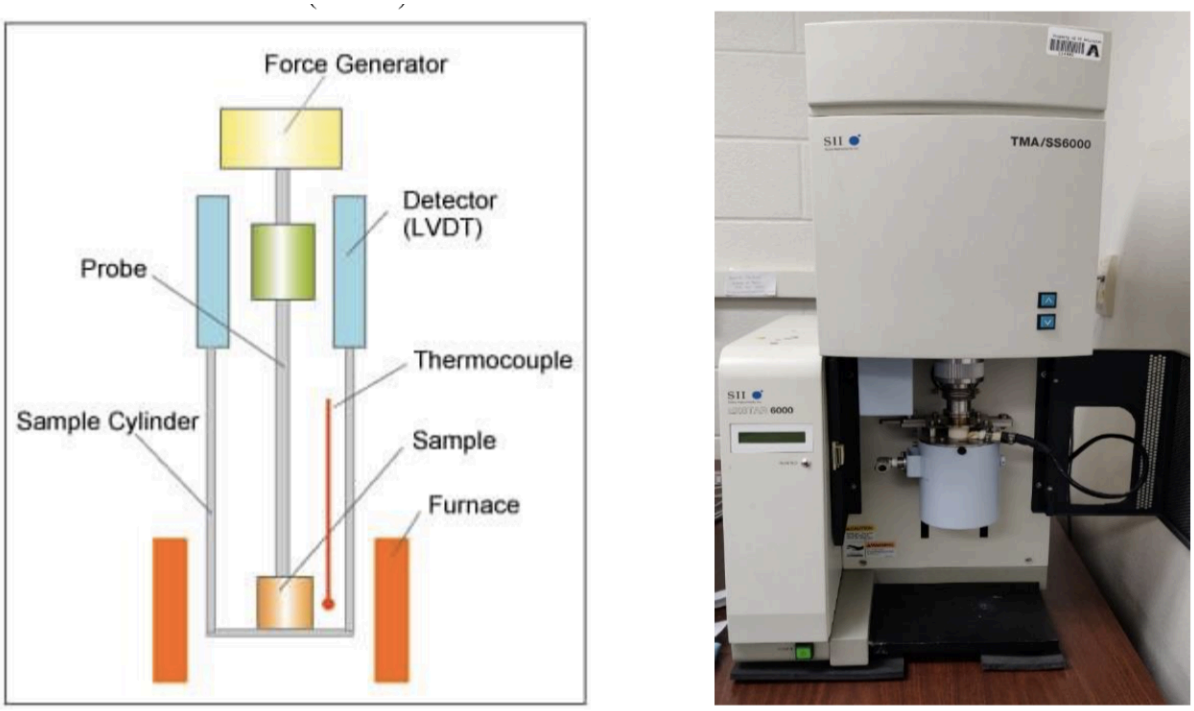

Figure 9 (a) Schematic of TMA (b)TMA

2.3 Dielectric Fluid

Dielectric is a very poor conductor or insulator of electric current. Dielectrics do not have loose bonds or free electrons unlike metals. When they are placed in the field the phenomenon called as dielectric polarization takes place. Because of dielectric polarization, the positive charges within the dielectric move slightly towards electric field and negative charges move slightly away from electric field. Hence, in case of dielectrics, conduction does not occur due to dielectric polarization and not because of the obstruction of flowability of electric charges. This property of dielectric liquid makes it perfect candidate for used as a coolant in direct contact with the electronic devices.[3]

Types of Dielectric fluid

1. Mineral Oil
2. Flurocarbon-based Fluids
3. Synthetic Fluids

For this experiments, dielectric fluid EC-100 was used. The applications of EC-100 include enterprise grade cooling of servers, GPU/CPU, semiconductors and electronics. Some of the key characteristics of EC-100 are low viscosity, high dielectric strength and good heat transfer capacity. It is non-compressible, isotropic, and Newtonian fluid [3].

Table 2 Data Sheet of EC-100

Characteristics	**Value**
Dielectric Strength (kV/mm2)	>40
Resistivity (ohm-cm)	>1014
Dielectric Constant	2.1
Pour Point (°C)	-42
Flash Point (°C)	160
Density (g/cc @ 16°C)	0.8
CTE (Vol/°C)	0.00065
Viscosity (cSt) @ 0°C	27.44

Viscosity (cSt) @ 40°C	5.30
Viscosity (cSt) @ 100°C	2.00
Thermal Conductivity (W/m°K) @ 0°C	0.1382
Thermal Conductivity (W/m°K) @ 40°C	0.1359
Thermal Conductivity (W/m°K) @ 100°C	0.1325
Sp. Heat (kJ/kg°C) @ 0°C	2.0608
Sp. Heat (kJ/kg°C) @ 40°C	2.2121
Sp. Heat (kJ/kg°C) @ 100°C	2.4388
Global Warming Potential	0
Biodegradability (28 days)	>93%
Materials Compatibility warranty	Yes
Product Operational Warranties (Yrs)	0.5
Shelf Life (Yrs)	25

2.4 PCB

185HR: 185 HR laminate and prepreg materials are a proprietary, high performance resin system with a Tg of 180°C for multilayer Printing Wiring Board (PWB) applications where maximum thermal performance and reliability are required [15].

185HR laminate and prepreg materials are manufactured reinforced with electrical grade (E-glass) glass fabric. This system delivers a 340°C decomposition temperature, a lower Z-axis expansion and offers lower loss compared to competitive products in this space. The 185HR system is also laser fluorescing and UV blocking for maximum compatibility with Automated Optical Inspection (AOI) systems, optical positioning systems and photoimageable solder mask imaging [15].

Table 3 Data Sheet of 185HR [15]

Property		Typical Value	Units	Test Method
			Metric (English)	IPC-TM-650 (or as noted)
Test data generated from rigid laminate		50	%	2.3.16.2
Glass Transition Temperature (Tg) by DSC		180	°C	2.4.25C
Glass Transition Temperature (Tg) by DMA		185	°C	2.4.24.4
Decomposition Temperature (Td) by TGA @ 5% weight loss		340	°C	2.4.24.6
Property		Typical Value	Units	Test Method
			Metric (English)	IPC-TM-650 (or as noted)
Time to Delaminate by TMA (Copper removed)	. T260 . T288	60 >15	Minutes	2.4.24.1

Thermal Conductivity		0.4	W/mK	ASTM E1952
Thermal Stress 10 sec @ 288ºC (550.4ºF)	. Unetched . Etched	Pass	Pass Visual	2.4.13.1
Dk, Permittivity	. @ 100 MHz . @ 1 GHz . @ 2 GHz . @ 5 GHz . @ 10 GHz	4.13 4.04 4.01 3.88 3.88	—	2.5.5.3 Bereskin Stripline Bereskin Stripline Bereskin Stripline Bereskin Stripline
Df, Loss Tangent	. @ 100 MHz . @ 1 GHz . @ 2 GHz . @ 5 GHz	0.0158 0.0192 0.0200 0.0235	—	2.5.5.3 Bereskin Stripline Bereskin Stripline

370HR: 370HR is the industry's "best in class" lead-free compatible product for high-reliability applications across a wide range of markets.

370HR laminates and prepregs are made using a patented high performance 180°C Tg FR-4 multi-functional epoxy resin system that is designed for multi-layer Printed Wiring Board (PWB) applications where maximum thermal performance, reliability superior CAF resistance are

required. This system provides superior thermal performance with low Coefficient of Thermal Expansion (CTE) and the mechanical, chemical and moisture resistance properties that equal or exceed the performance of traditional FR-4 materials [16].

370HR is used in thousands of PWB designs and has proven to be best in class for thermal reliability, CAF performance, ease of processing and proven performance on sequential lamination designs [16].

Table 4 Data Sheet of 370HR [16]

Property		Typical Value	Units	Test Method
			Metric (English)	IPC-TM-650 (or as noted)
Glass Transition Temperature (Tg) by DSC		180	°C	2.4.25C
Decomposition Temperature (Td) by TGA @ 5% weight loss		340	°C	2.4.24.6
Time to Delaminate by TMA (Copper removed)	. T260 . T288	60 30	Minutes	2.4.24.1
Thermal Conductivity		—	W/mK	ASTM E1952
Thermal Stress 10 sec @ 288ºC (550.4ºF)	. Unetched . Etched	Pass	Pass Visual	2.4.13.1

Dk, Permittivity	. @ 100 MHz . @ 1 GHz . @ 2 GHz . @ 5 GHz . @ 10 GHz	4.24 4.17 4.04 3.92 3.92	—	2.5.5.3 2.5.5.9 Bereskin Stripline Bereskin Stripline Bereskin Stripline
Df, Loss Tangent	. @ 100 MHz . @ 1 GHz . @ 2 GHz . @ 5 GHz . @ 10 GHz	0.0150 0.0161 0.0210 0.0250 0.0250	— — — 	2.5.5.3 2.5.5.9 Bereskin Stripline 2.5.5.5 2.5.5.5
Volume Resistivity	. After moisture resistance . At elevated temperature	3.0×10^8 7.0×10^8	MΩ-cm	2.5.17.1
Surface Resistivity	. After moisture resistance . At elevated temperature	3.0×10^6 2.0×10^8	MΩ	2.5.17.1
Dielectric Breakdown		>50	kV	2.5.6B

Arc Resistance	115	Seconds	2.5.1B

Electric Strength (Laminate & laminated prepreg)		54 (1350)	kV/mm (V/mil)	2.5.6.2A
Comparative Tracking Index (CTI)		3 (175-249)	Class (Volts)	UL 746A ASTM D3638
Peel Strength	. Low profile copper foil and very low-profile copper foil all copper foil >17 µm [0.669 mil] . Standard profile copper 1. After thermal stress 2. At 125ºC (257ºF) 3. After process solutions	1.14 (6.5) 1.25 (7.0) 1.25 (7.0) 1.14 (6.5)	N/mm (lb/inch)	2.4.8C 2.4.8.2A 2.4.8.3 2.4.8.3
Flexural Strength	. Length direction . Cross direction	90.0 77.0	ksi	2.4.4B
Test data generated from rigid laminate	. Length direction . Cross direction	3744 3178	ksi	ASTM D790-15e2
Poisson's Ratio	. Length direction . Cross direction	0.177 0.171	—	ASTM D3039
Moisture Absorption		0.15	%	2.6.2.1A
Flammability (Laminate & laminated prepreg)		V-0	Rating	UL 94

Max Operating Temperature	130	°C	UL 796

2.5 Experimental Procedure

Twelve PCB samples were prepared for each 185HR and 370HR. These 7mm*7mm samples were cut using high speed cutter. After cutting, sample edges were polished by fine polish paper to remove unevenness. Samples were thoroughly cleaned with ethanol to remove the dust particles. Four samples of each type were kept without immersion at room temperature for comparison purposes. Four samples of each type were immersed in EC-100 at room temperature. Four samples of each type were immersed in EC-100 at 125°C for thermal aging. Total twenty-four samples were kept for duration of 720 hours.

After 720 hours, PCB samples were gently swept to remove EC-100 layer on sample surfaces to get accurate results. All samples were tested within a duration of three days after sample were removed from EC-100. Thermo-Mechanical Analyzer (TMA) was used to measure CTE and glass transition temperature of the samples. In-plane CTE was calculated using compression probe in TMA. Before the measurements of samples, TMA was calibrated using Al cylinder to verify accuracy of the machine. Samples were tested for temperature range of 25°C to 220°C. Each test took approximately 75 minutes. For each case, average values were taken for the measured CTE.

Chapter 3

Experimental Results

3.1 Experimental CTE Results of 185HR PCB

Following graph shows CTE measurements of 185HR PCB samples in case of pre immersion. The graph includes measurements from 25°C to 220°C.

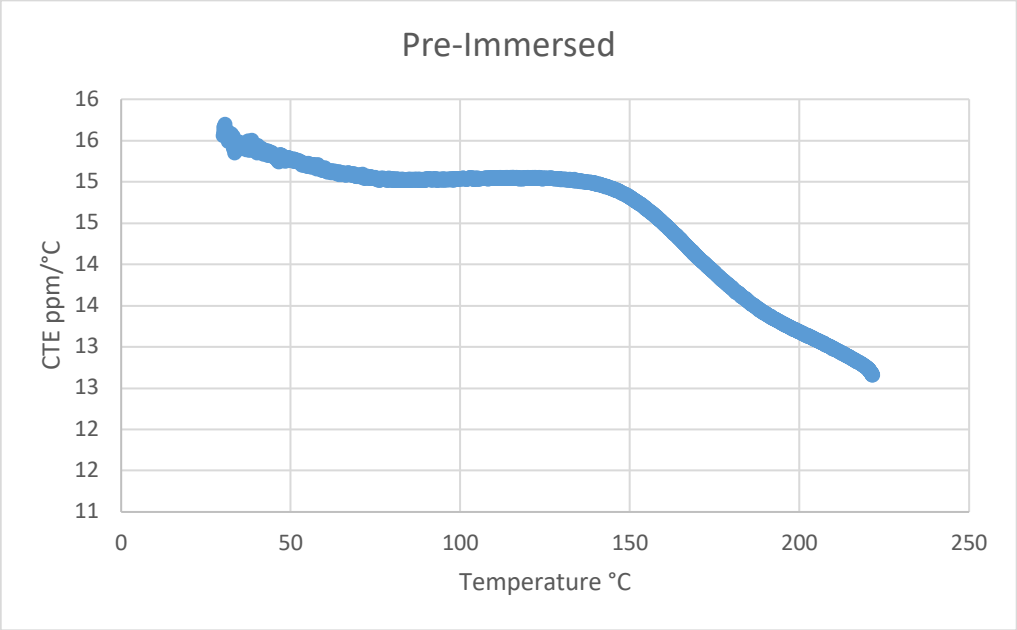

Figure 10 CTE of Pre-Immersed 185HR PCB

Following graph shows CTE measurements of 185HR PCB samples in case of post immersion at room temperature. The graph includes measurements from 25°C to 220°C.

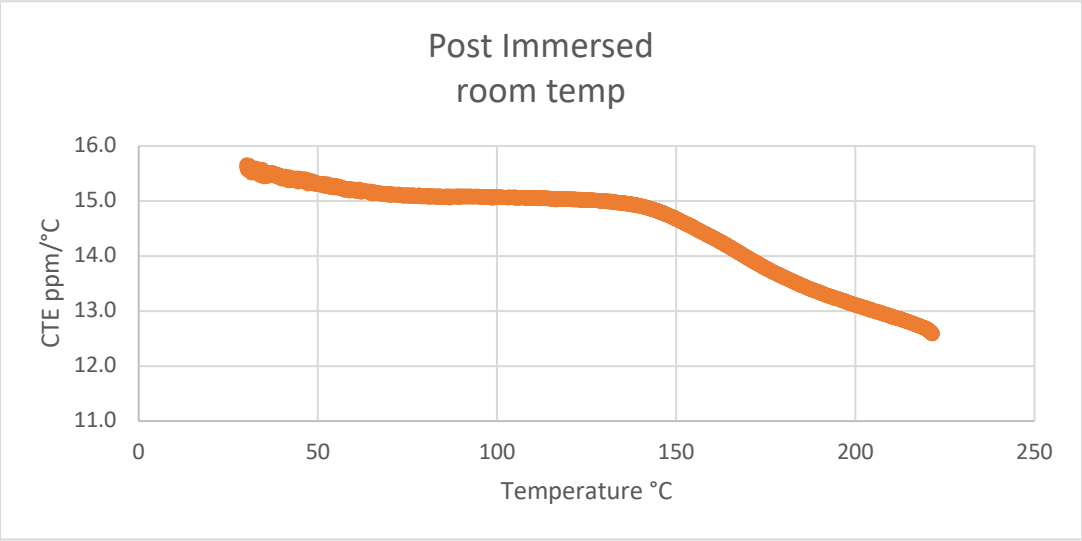

Figure 11 CTE of Post-Immersed (Room Temperature) 185HR PCB

Following graph shows CTE measurements of 185HR PCB samples in case of post immersion at 125°C. The graph includes measurements from 25°C to 220°C.

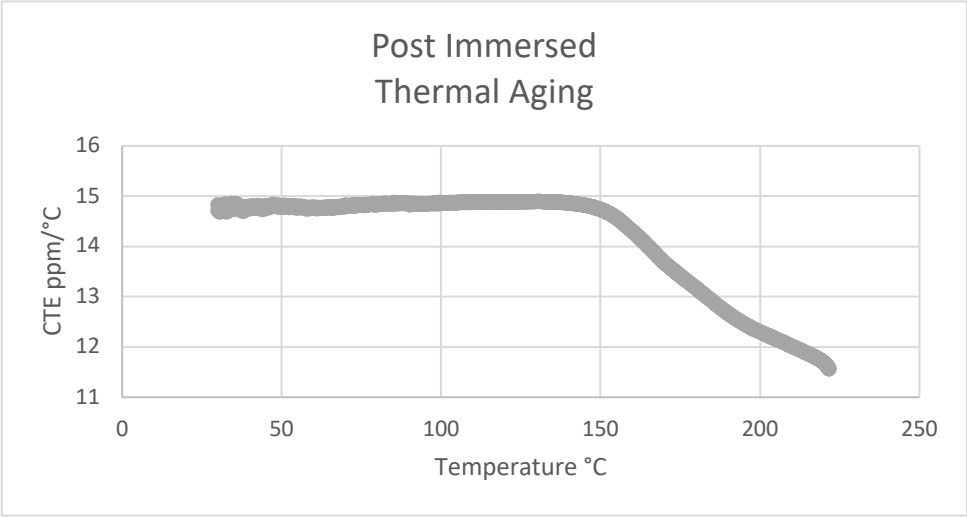

Figure 12 CTE of Post-Immersed (Thermal Aging) 185HR PCB

Following graph shows comparison CTE measurements of 185HR PCB samples in all three cases. The graph includes measurements from 25°C to 220°C.

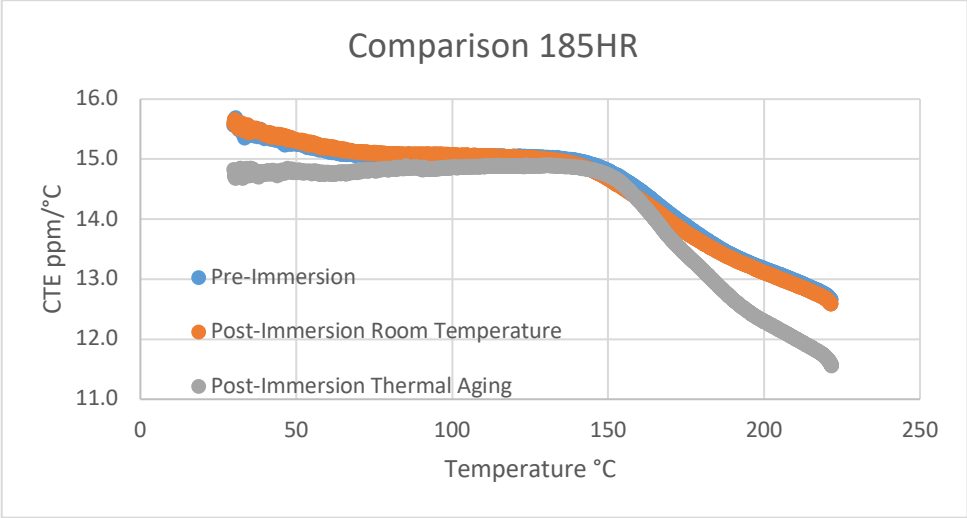

Figure 13 Comparison of CTEs of 185HR PCB

3.2 Experimental CTE Results of 370HR PCB

Following graph shows CTE measurements of 370HR PCB samples in case of pre immersion. The graph includes measurements from 25°C to 220°C.

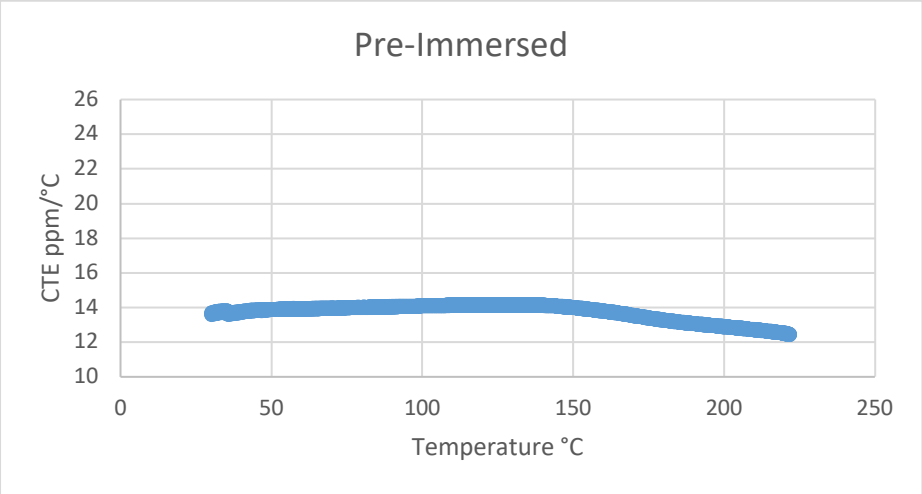

Figure 14 CTE of Pre-Immersed 370HR PCB

Following graph shows CTE measurements of 370HR PCB samples in case of post immersion at room temperature. The graph includes measurements from 25°C to 220°C.

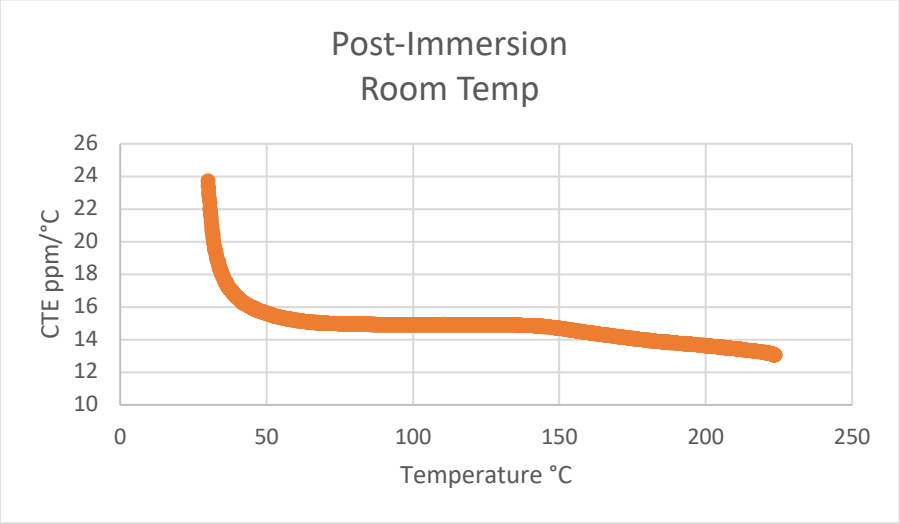

Figure 15 CTE of Post-Immersed 370HR PCB

Following graph shows CTE measurements of 370HR PCB samples in case of post immersion at 125°C. The graph includes measurements from 25°C to 220°C.

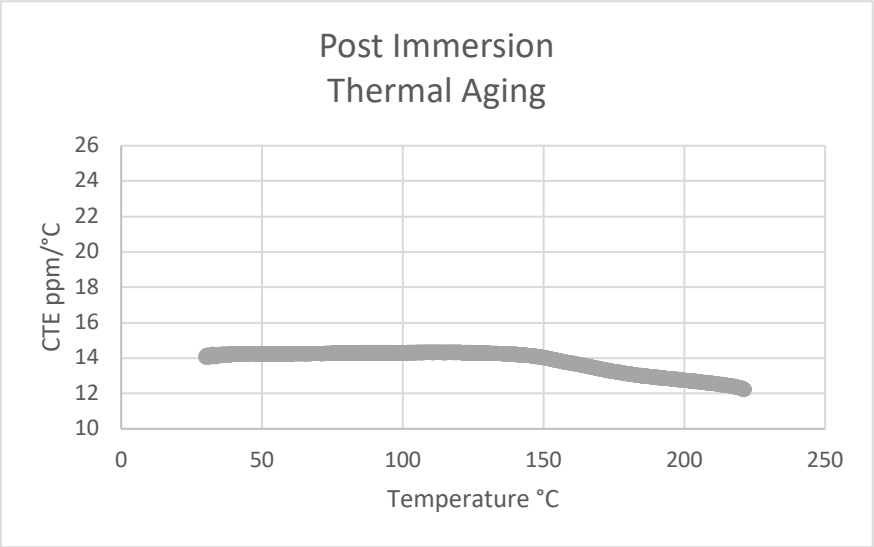

Figure 16 CTE of Post-Immersed (Thermal Aging) 370HR PCB

Following graph shows comparison of CTE measurements of 370HR PCB samples for all three cases. The graph includes measurements from 25°C to 220°C.

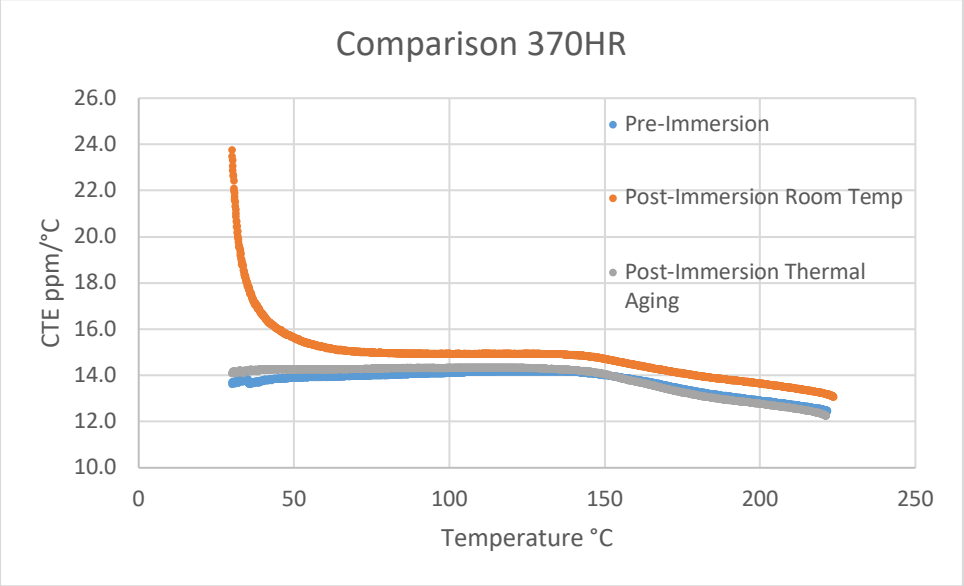

Figure 17 Comparison of CTEs of 370HR PCB

3.3 Result Discussion

As CTE mismatch is one of the most crucial factors in 2nd level solder joint reliability, data regarding change in CTE of different components after immersion is important step in adopting single phase immersion cooling widely. Change in CTE could lead to either increase in CTE mismatch reducing solder fatigue life or decrease in CTE mismatch increasing solder fatigue life. Presented experimental data shows the results of CTE for both PCBs 185HR and 370HR in case of all three experiments (1) Pre-Immersion room temp; (2) Post-Immersion room temp; (3) Post-Immersion thermal aging have no significant change.

Chapter 4

Modelling and FE Analysis

4.1 Model Description

Ball Grid Array (BGA) Package is a type of surface mount technology package. BGA package has a greater number of interconnects and hence good connectivity with lower thermal resistance. TI-ZQZ BGA model with 120 solder balls was used for the simulations[25].

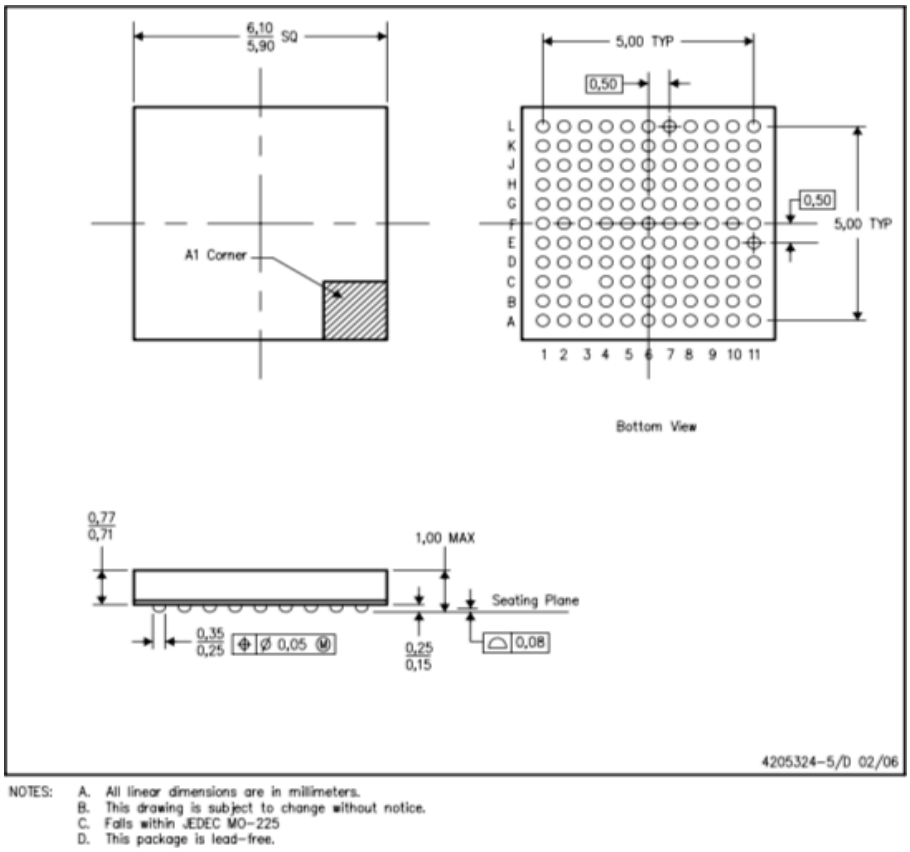

Figure 18 Schematic of BGA Package

Figure shows descriptive BGA model with its components. On both top and bottom side of the solder ball copper pad is placed. On the top side of solder balls i.e. substrate side, the silicon die is attached to polyimide layer with an adhesive layer sandwiched between the two. On both, the PCB side and the substrate side solder mask is present as shown in the schematic.

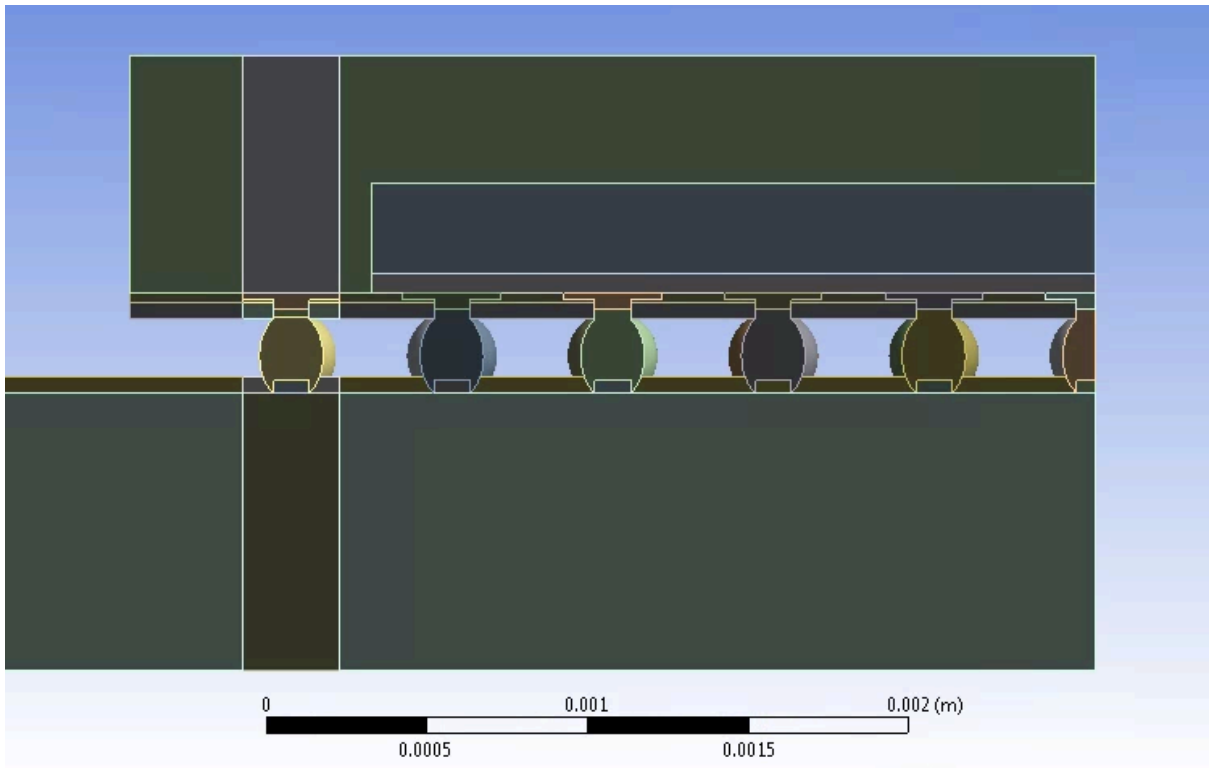

Figure 19 ANSYS Workbench BGA Model

Table 5 Material Properties

Material	**E (GPa)**	**Poisson's Ratio (υ)**	**CTE (ppm/°C)**
Adhesive	8.737	0.4	14.6
Solder Mask	4.137	0.4	52
Die	150	0.28	2.9
Mold	24	0.35	20
Cu Pad	127	0.34	16.7
Die Attach	1.54	0.35	65
Pi Layer	3.3	0.4	35

4.2 Computational Analysis

Finite Element Analysis is used to for computational analysis. In this case, octant symmetric model exists, hence it was used to save computational time. Symmetric boundary conditions were used at the split sections of octant symmetric model [19]. All the properties of components are considered linear elastic except solder balls. Various researchers are working to determine anisotropic elastic properties of coarse-grained SAC305 solder joints. As solder balls are highly anisotropic, each ball has a unique grain structure and hence unique elastic properties. Therefore, data for these properties is important from a package reliability perspective [20]. To predict visco-plastic behavior of solder balls, Anand Constants were used [21].

Anand viscoplastic constitutive model is popular as it uses both plasticity and creep. Viscoplastic constitutive equations for rate dependent deformations are used to find fatigue life. In this model, isotropic resistance to plastic flow is represented by scalar internal variable "S". The creep and rate dependent plastic behavior of solder is unified using flow equation, stress equation and evolution equation. The Anand model does not need either explicit yield condition or loading/unloading criterion [21].

$$\frac{d\varepsilon_p}{dt} = \text{Asinh}\left(\xi\frac{\sigma}{s}\right)^{\frac{1}{m}} \exp\left(-\frac{Q}{kT}\right)$$

$$\dot{s} = [h_0(|B|)^{\propto}\frac{B}{|B|}]\frac{d\varepsilon_p}{dt}$$

$$B = 1 - \frac{s}{s^*}$$

$$s' = \hat{s}\left[\frac{1}{A}\frac{d\varepsilon_p}{dt}\exp\left(-\frac{Q}{kT}\right)\right]^n$$

In this work nine Anand constants calculated from creep test data measured at several stress levels by Motalab, et al are used [21].

Table 6 Anand Constants for SAC305 [21]

Variable	**SAC305**
S_o (MPa)	18.07
Q/R (1/K)	9096
A (1/s)	3484
E	4.0
M	0.20
h_o (MPa)	144,000
S (MPa)	26.4
n	0.01
a	1.90

4.3 Methodology and Meshing

Common modelling techniques used in electronic packaging are;

1. Nonlinear slice model
2. Nonlinear global model with super elements
3. Linear global model with sub-model

4. Nonlinear global model with a sub-model

5. Nonlinear global model

In this study, nonlinear global model with sub-model was used. Critical solder joint is identified based on maximum difference of either total or vertical displacement of top and bottom of the solder balls [22].

In FE Analysis, larger the number of elements, better is the approximation. Though in some cases, excessive number of elements may cause error. Mesh sensitivity analysis is a technique used to find converged results. Initially course meshing is done, and then finer mesh is done mainly on the identified critical parts till the results are converged [21].

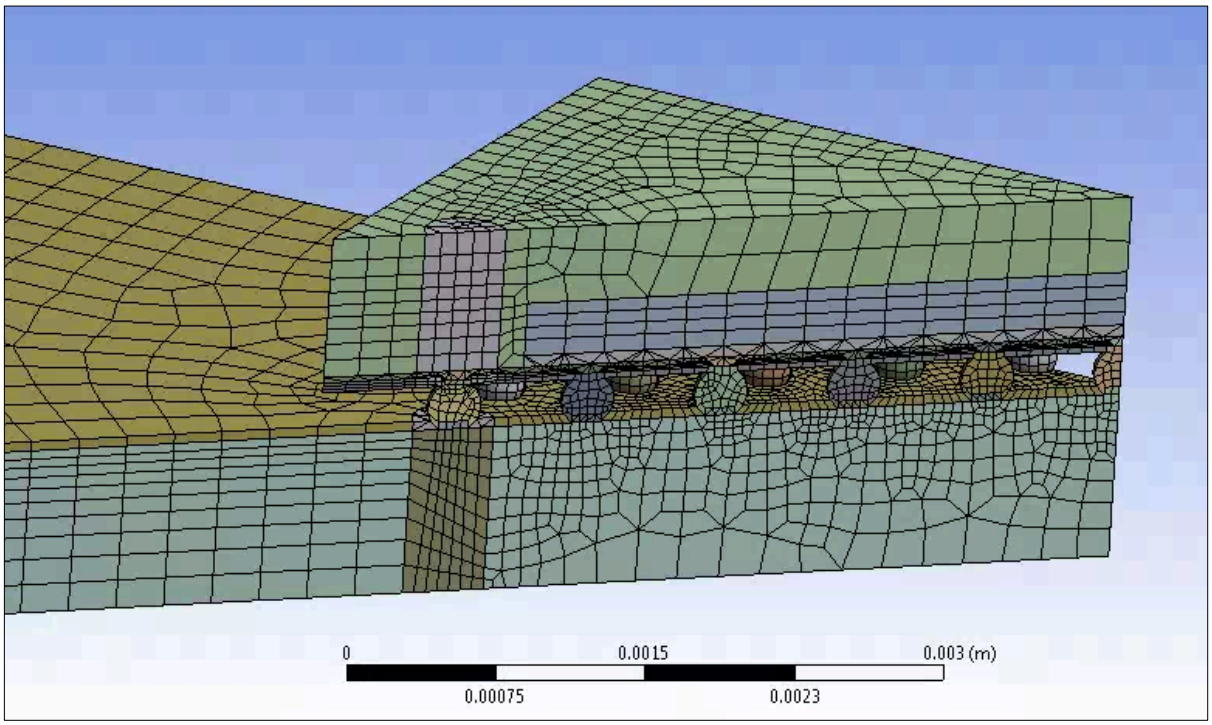

Figure 20 Meshed ANSYS Workbench Model

4.4 Load and Boundary Conditions

Symmetric boundary condition is applied on edge surfaces of octant symmetric model. Center node of the package is fixed to prevent rigid body translation in all directions. From JEDEC JESD22-A104D, thermal cycling was used. Three thermal cycles were applied from -40°C to 125°C with 15 minutes of ramp and 15 minutes of dwell. Total duration of each cycle was 60 minutes. Three cycles are used as minimum three cycles are required to obtain a stable stress-strain hysteresis loop [23]. In sub-model, the corresponding cut-boundary displacement conditions are applied to the interfaces between global and sub-model.[22]

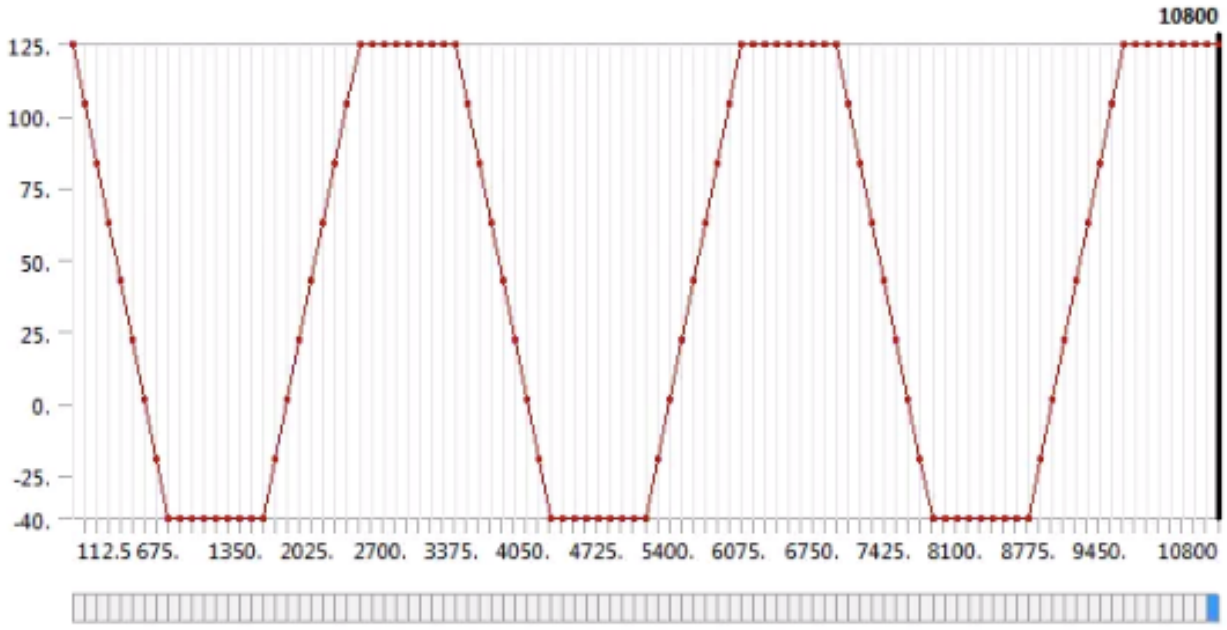

Figure 21 ATC Profile

Chapter 5

Simulation Results

5.1 Results

Corner solder ball is identified as critical solder ball. Maximum equivalent (Von-Mises) stress, maximum total deformation, non-linear plastic work and plastic work difference for each cycle was calculated.

185HR PCB:

Following graph shows maximum equivalent stress developed in corner solder ball at the end of third cycle. The change in maximum equivalent stress is less than 1%.

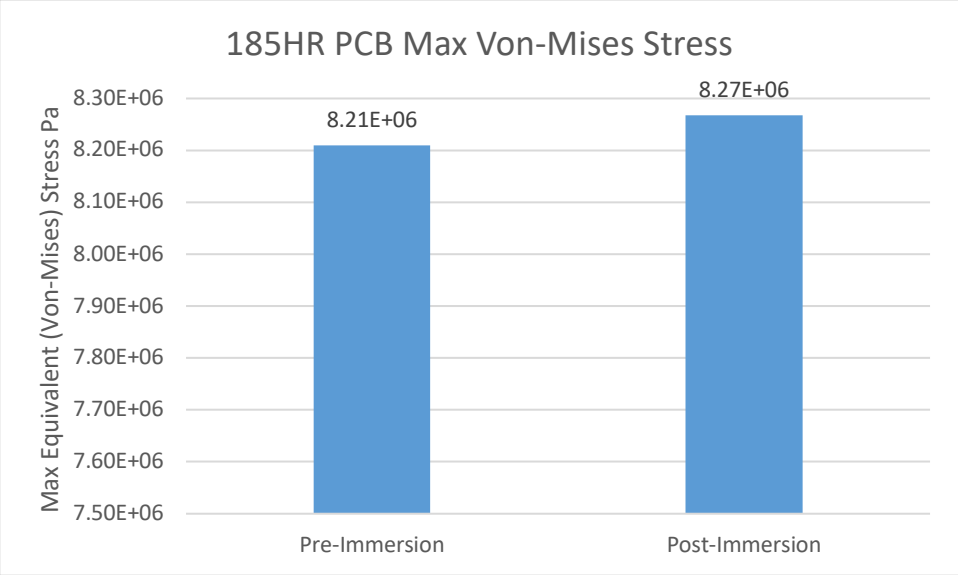

Figure 22 Max Equivalent Stress 185HR PCB

Following graph shows maximum total deformation on corner solder ball for pre-immersion and post-immersion. The increase in total deformation is around 6%.

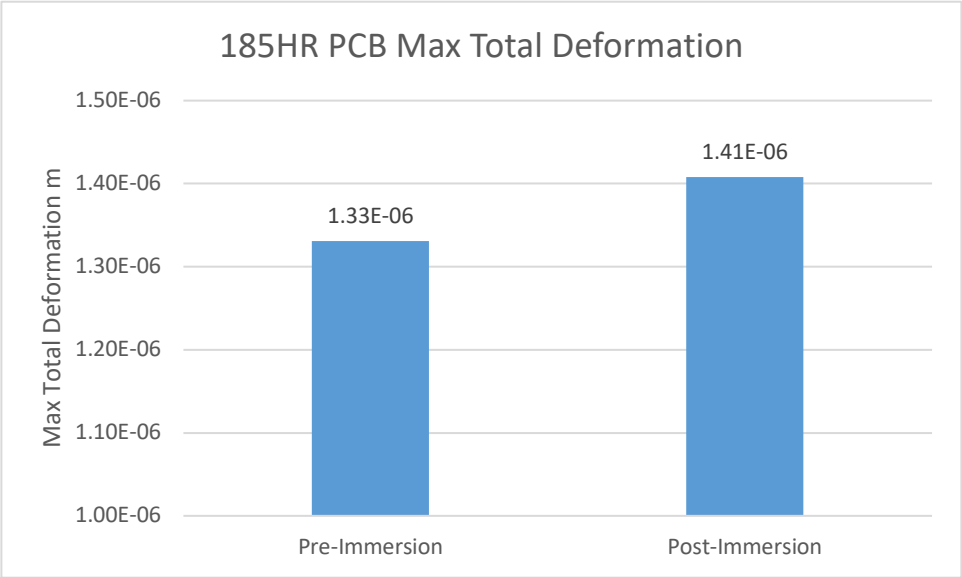

Figure 23 Maximum Total Deformation 185HR PCB

Following graph shows maximum nonlinear plastic work on corner solder ball. It is decreased by 0.8% after immersion.

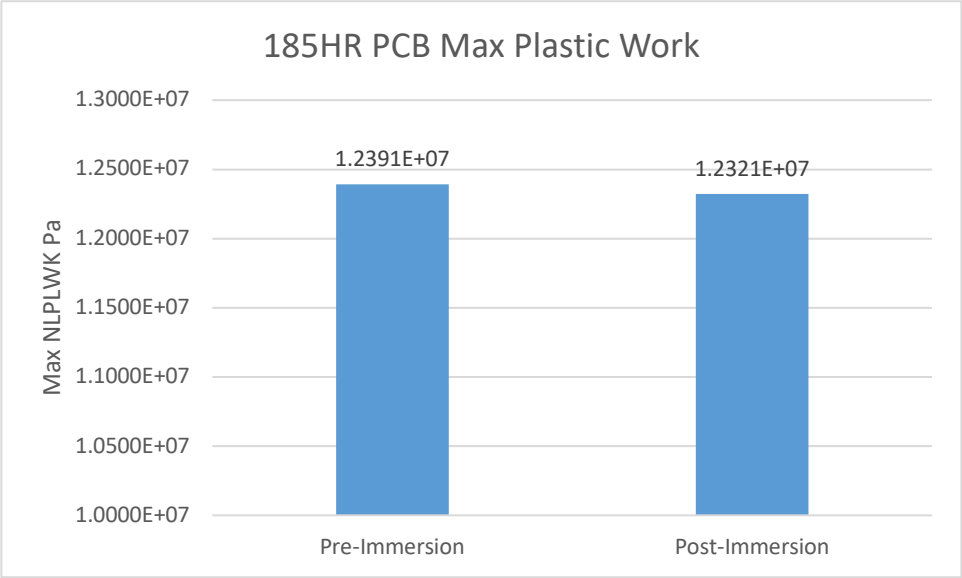

Figure 24 Maximum Non-Linear Plastic Work 185HR PCB

Following graph shows the comparison between plastic work difference for last cycle for pre-immersion and post-immersion 185HR PCB values. In this case, plastic work difference is reduced by 2.7%.

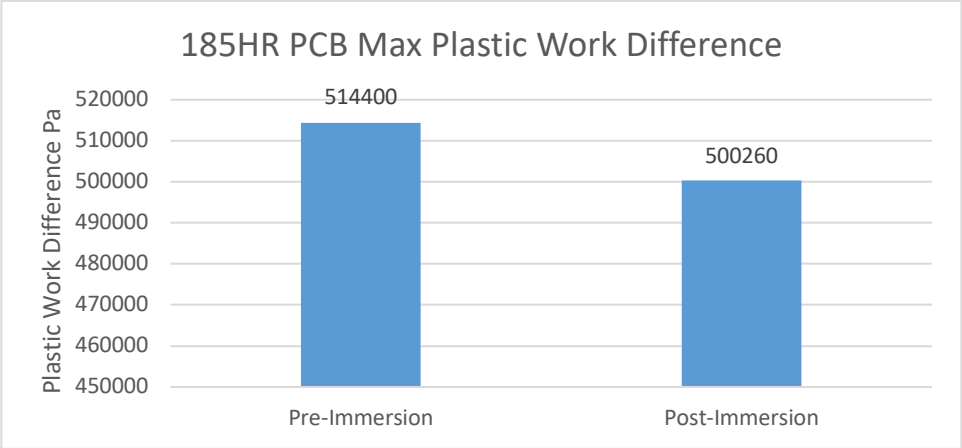

Figure 25 Plastic Work Difference 185HR PCB

370HR PCB:

Following graph shows maximum equivalent stress developed in corner solder ball at the end of third cycle. The change in maximum equivalent stress is around 1%.

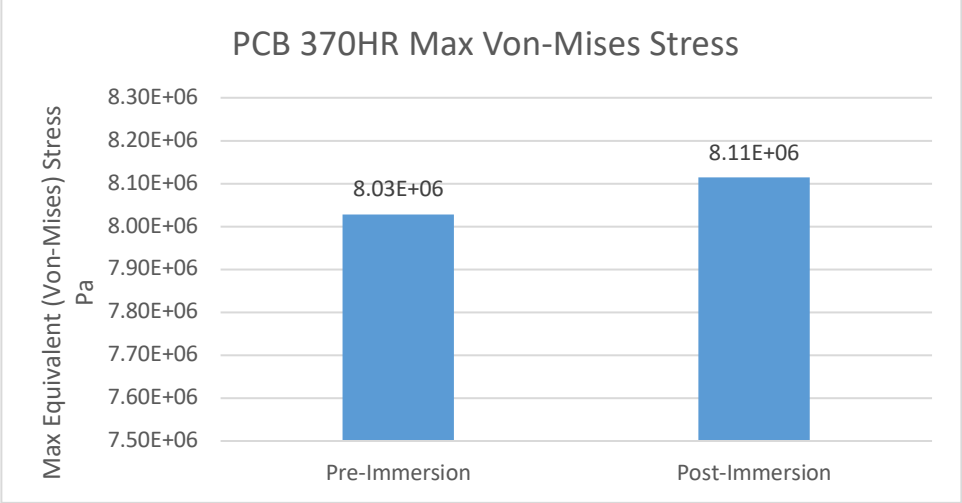

Figure 26 Maximum Equivalent Stress 370HR PCB

Following graph shows maximum total deformation on corner solder ball for pre-immersion and post-immersion. The increase in total deformation is around 7%.

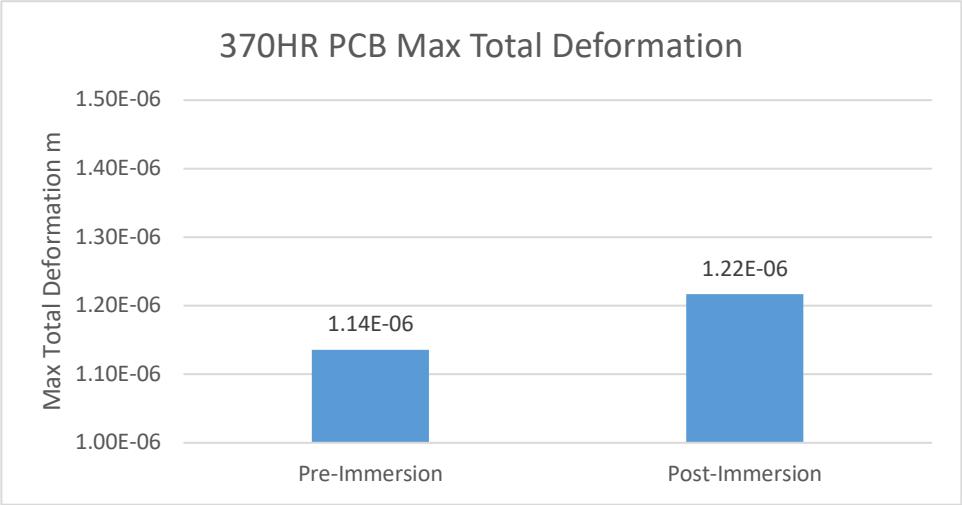

Figure 27 Maximum Total Deformation 370HR PCB

Following graph shows maximum nonlinear plastic work on corner solder ball. It is decreased by 4.4% after immersion.

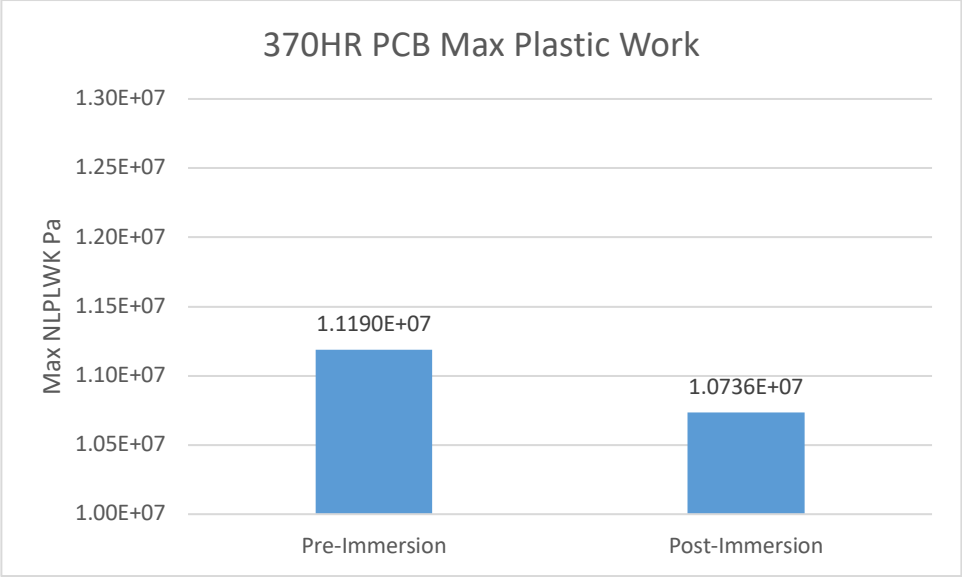

Figure 28 Maximum Non-Linear Plastic Work 370HR

Following graph shows the comparison between plastic work difference for last cycle for pre-immersion and post-immersion 370HR PCB values. In this case, plastic work difference is reduced by 5.3%.

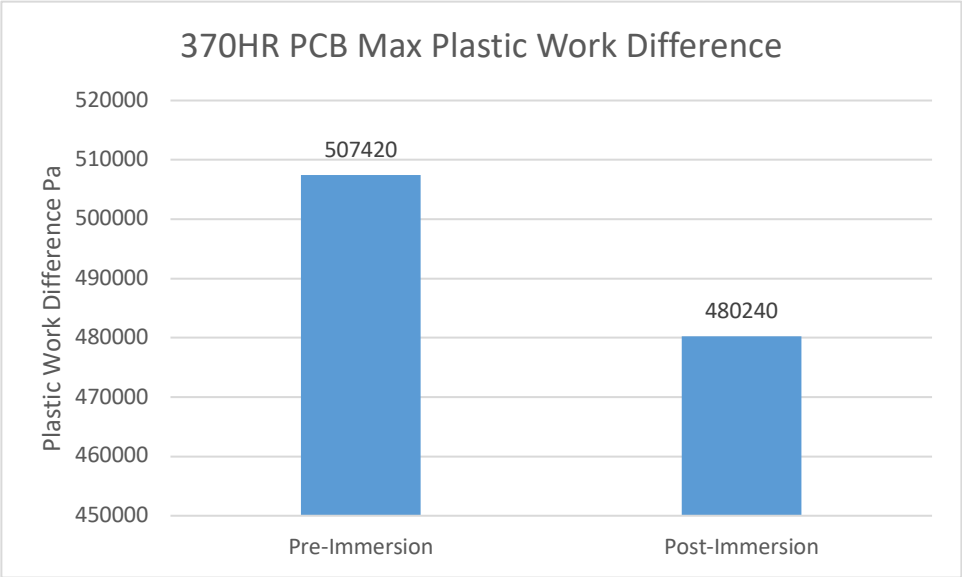

Figure 29 Plastic Work Difference 370HR

5.2 Result Discussion

The main purpose of simulations was to observe impact of change in CTE and Young's Modulus PCB after immersion on solder fatigue life. As there is no change in CTE of PCB after immersion, change in modulus plays major part on impact on 2nd level solder joint reliability. The Young's Modulus is decreasing after immersion. Decrease in stiffness has shown improvement plastic work difference and hence solder fatigue life.

Chapter 6

Conclusion and Future Work

6.1 Conclusion

The experimental results of CTE for both 185HR PCB and 370HR PCB in case of all three experiments (1) Pre-Immersion room temp; (2) Post-Immersion room temp; (3) Post-Immersion thermal aging shows no significant difference to each other. As CTE mismatch is one of the most concerning reliability issues, these results are positive start for further research and hence for adoption of single-phase immersion cooling from reliability point of view.

The simulation results show that plastic work difference is decreasing after immersion for both 185HR PCB and 370HR PCB. As plastic work difference is directly proportional to solder fatigue life, we can conclude that solder joint reliability is improved after immersion. The cause of improved reliability is mainly the decrease of complex modulus of PCBs after immersion.

6.2 Future Work

1. TGA study for same 185HR and 370HR PCB samples to investigate amount of oil absorbed.
2. Similarly, effect of immersion on various package components by measuring CTE, Young's Modulus and amount of oil absorbed using TMA, DMA and TGA respectively.
3. Along with room temperature immersion and thermal aging, thermal cycling will give more realistic data information.
4. Package components can be individually tested and can be tested in a bulk to study change in properties and impact of individual components on assembly.

REFERENCES

[1] "What Is Data Center" By Paloalto Networks

[2] "The Digital Universe In 2020: Big Data, Bigger Shadows And Biggest Growth In The Far East" By IDC Dec 2012

[3] The Editors Of Encyclopaedia Britannica, "Dielectric"

[4] Submer, "What Is Immersion Cooling" Submer.Com

[5] Fangzhi, 'Immersion Cooling For Green Computing', Alibaba Group, OCP Summit, 2018

[6] Shah, J. M., Eiland, R., Rajmane, P., Siddarth, A., Agonafer, D., And Mulay, V. (April 10, 2019). "Reliability Considerations For Oil Immersion-Cooled Data Centers." ASME. J. Electron. Packag. June 2019; 141(2): 021007. Https://Doi.Org/10.1115/1.4042979

[7] David W. Sundin"Mineral Oil, White Oil And Synthetic Dielectric Coolants; How Engineered Fluids' Dielectric Coolants Differ From Petroleum Based Dielectric Oil" Engineered Fluids, LLC. / October 23, 2017, Https://Www.Engineeredfluids.Com/Immersioncooling"

[8] "Immersion Cooling For Data Centers" 3m.Com

[9] West, Bob "Understanding The Interplay Between Data Center Power Consumption/Data Center Energy Consumption And Power Density" Datacenters.Com

[10] "Comparison Between Data Center Liquid Cooling Solutions"- Paolo Bianco

[11] Lohia, Alok Kumar," Optimization Of Board Level Reliability Of Microelectronic Packages And Modules ", UTA Dissertation, Https://Hdl.Handle.Net/10106/27554

[12] Rahangdale, Unique " Structural Optimization & Reliability Of 3d Package By Studying Crack Behavior On Tsv & Beol & Impact Of Power Cycling On Reliability Flip Chip Package ", UTA Thesis Http://Hdl.Handle.Net/10106/27317

[13] Karnik, Anuraag, " Impact Of Thermal Aging On Crack Growth Behavior Of Lead Free Solder Interconnects " UTA Thesis, Http://Hdl.Handle.Net/10106/27480

[14] Rajmane, Pavan, Mirza, Fahad, Khan, Hassaan, And Agonafer, Dereje. "Chip Package Interaction Study To Analyze The Mechanical Integrity Of A 3-D TSV Package." Proceedings Of The ASME 2015 International Technical Conference And Exhibition On Packaging And Integration Of Electronic And Photonic Microsystems Collocated With The ASME 2015 13th International Conference On Nanochannels, Microchannels, And Minichannels. Volume 2: Advanced Electronics And Photonics, Packaging Materials And Processing; Advanced Electronics And Photonics: Packaging, Interconnect And Reliability; Fundamentals Of Thermal And Fluid Transport In Nano, Micro, And Mini Scales. San Francisco, California, USA. July 6–9, 2015. V002T02A009. ASME. Https://Doi.Org/10.1115/IPACK2015-48811

[15] Isola Group "185HR Data Sheet" Https://Www.Isola-Group.Com/Wp-Content/Uploads/Data-Sheets

[16] Isola Group "370HR Data Sheet" Https://Www.Isola-Group.Com/Wp-Content/Uploads/Data-Sheets

[17] Ramdas, Shrinath, Rajmane, Pavan, Chauhan, Tushar, Misrak, Abel, And Agonafer, Dereje. "Impact Of Immersion Cooling On Thermo-Mechanical Properties Of PCB's And Reliability Of Electronic Packages." Proceedings Of The ASME 2019 International Technical Conference And Exhibition On Packaging And Integration Of Electronic And Photonic Microsystems. ASME 2019 International Technical Conference And Exhibition On Packaging And Integration Of Electronic And Photonic Microsystems. Anaheim, California, USA. October 7–9, 2019. V001T02A011. ASME. Https://Doi.Org/10.1115/IPACK2019-6568

[18] A. Deshpande, Q. Jiang, A. Dasgupta And U. Becker, "Fatigue Life Of Joint-Scale SAC305 Solder Specimens In Tensile And Shear Mode," 2019 18th IEEE Intersociety Conference On

Thermal And Thermomechanical Phenomena In Electronic Systems (Itherm), Las Vegas, NV, USA, 2019, Pp. 1026-1029, Doi: 10.1109/ITHERM.2019.8757405.

[19] Rajmane, Pavan, Mirza, Fahad, Khan, Hassaan, And Agonafer, Dereje. "Chip Package Interaction Study To Analyze The Mechanical Integrity Of A 3-D TSV Package." Proceedings Of The ASME 2015 International Technical Conference And Exhibition On Packaging And Integration Of Electronic And Photonic Microsystems Collocated With The ASME 2015 13th International Conference On Nanochannels, Microchannels, And Minichannels. Volume 2: Advanced Electronics And Photonics, Packaging Materials And Processing; Advanced Electronics And Photonics: Packaging, Interconnect And Reliability; Fundamentals Of Thermal And Fluid Transport In Nano, Micro, And Mini Scales. San Francisco, California, USA. July 6–9, 2015. V002T02A009. ASME. Https://Doi.Org/10.1115/IPACK2015-48811

[20] Jiang, Q., Deshpande, A. & Dasgupta, A. Elastic Behavior Of Coarse-Grained Snagcu (SAC) Solder Joints Based On An Anisotropic Multi-Scale Predictive Modeling Approach. Journal Of Elec Materi 48, 8076–8088 (2019). Https://Doi.Org/10.1007/S11664-019-07576-X

[21] M. Motalab, Z. Cai, J. C. Suhling And P. Lall, "Determination Of Anand Constants For SAC Solders Using Stress-Strain Or Creep Data," 13th Intersociety Conference On Thermal And Thermomechanical Phenomena In Electronic Systems, San Diego, CA, 2012, Pp. 910-922, Doi: 10.1109/ITHERM.2012.6231522.

[22] G. Gustafsson, I. Guven, V. Kradinov And E. Madenci, "Finite Element Modeling Of BGA Packages For Life Prediction," 2000 Proceedings. 50th Electronic Components And Technology Conference (Cat. No.00CH37070), Las Vegas, NV, USA, 2000, Pp. 1059-1063, Doi: 10.1109/ECTC.2000.853300.

[23] U. Rahangdale, P. Rajmane, A. Doiphode And A. Misrak, "Structural Integrity Optimization Of 3D TSV Package By Analyzing Crack Behavior At TSV And BEOL," 2017 28th Annual SEMI Advanced Semiconductor Manufacturing Conference (ASMC), Saratoga Springs, NY, USA, 2017, Pp. 201-208, Doi: 10.1109/ASMC.2017.7969230.

[24] Ramdas, Shrinath et. al " Impact of Thermal Aging on Thermomechanical Properties of Oil-Immersed Printed Circuit Boards" SMTA International Conference 09.22.2019

[25] Reliability Assessment of BGA Solder Joints - Megtron 6 VS FR4 Printed Circuit Boards" SMTA International 09.26.2019 Pp. 136-141 Doi: https://www.smta.org/knowledge/proceedings_abstract.cfm?PROC_ID=5412